Pergamon

Tetrahedron 57 (2001) 3521–3528

TETRAHEDRON

Effects of aryl and arylethynyl substituents at the 1-position on rotational barrier around C(sp)–C(sp^3) bonds and bending deformation of acetylenic carbons in bis(9-triptycyl)ethynes☆

Shinji Toyota,* Takao Yamamori and Toshiaki Makino

Department of Chemistry, Faculty of Science, Okayama University of Science, Ridaicho, Okayama 700-0005, Japan

Received 18 August 2000; accepted 22 November 2000

Abstract—The barriers to rotation around C(sp)–C(sp^3) single bonds in (1,4-dimethyl-9-triptycyl)(1-X-9-triptycyl)ethynes [X=phenyl, mesityl, phenylethynyl, or (1-naphthyl)ethynyl] were determined by the dynamic NMR method to examine the effect of nonspherically shaped aromatic substituents on the rotational barriers. The rotational barriers increase in the order of the pheny, arylethynyl and mesityl substituted compounds from 15.8 to 18.8 kcal/mol. This result suggests that not only the bulkiness but also the shape and flexibility of the substituents are important factors in determining the rotational barrier. Significant bending deformations of the acetylenic carbons (~166°) were found in the X-ray structures and the optimized structures by the MM2 calculations.

1. Introduction

While acetylene units have been frequently utilized as a rigid and linear fragment in the novel aromatic chemistry, the rotational isomerism of C(sp)–C bonds in alkynes has been much less studied than those of C–C bonds involving tetrahedral and trigonal carbons because of the extremely low rotational barriers.[2,3] The restricted rotation around C(sp)–C(sp^3) bonds was observed in bis(9-triptycyl)ethynes (BTE), where the two bulky substituents interacted with each other across the acetylene axis during the bond rotation (Scheme 1).[1,4,5] Careful kinetic measurements by the dynamic NMR technique[6] revealed that the rotational barriers were enhanced almost linearly with the steric size of the 1′-substituent (X) in (1,4-dimethyl-9-triptycyl)(1-X-9-triptycyl)ethynes (**1**–**4**) for spherical or pseudospherical substituents (H, OMe, Me, F, Cl, Br and I) in the range 10.1–17.3 kcal/mol.[1,5]

We became interested in the effect of nonspherically shaped substituents containing aromatic groups on the rotational barriers in the BTE system. For these groups, various structural factors—shape, conformation and flexibility—should influence the total steric effect in the dynamic process. If the structures of the substituents are appropriately designed, further enhancement of the rotational barrier will be possible. Therefore, we studied compounds **5a**–**d** carrying phenyl, mesityl (Mes), phenylethynyl, or (1-naphthyl)-ethynyl group at the 1′-position, respectively, by spectroscopic methods. Because of the severe steric congestion, the molecules are subjected to structural deformation as shown by the X-ray analysis and the MM2 calculation. Especially, the bending deformation of the acetylenic carbons is discussed in relation to the rotational isomerism.

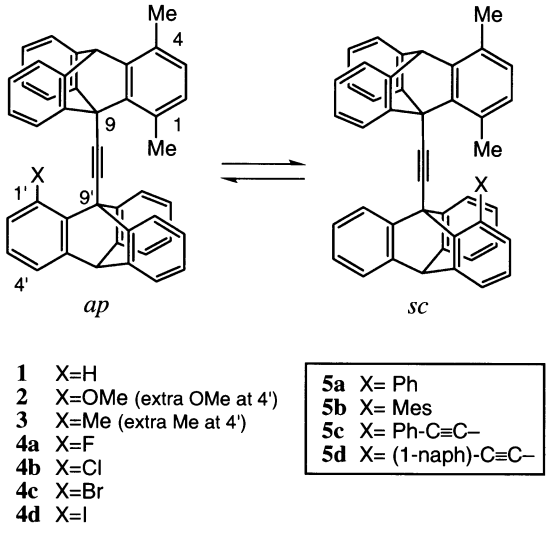

Scheme 1. Rotational isomerization in bis(9-triptycyl)ethynes (only one enantiomeric form is shown for the *sc* isomer. The *ap* and *sc* forms are

2. Results

The synthetic route to compounds **5** is basically the same as

☆ For Parts 2 and 3 of the series see Ref. 1.

Keywords: substituent effect; steric and strain effect; alkynes; stereoisomerism.

* Corresponding author. Tel./fax: +81-86-256-9457;
e-mail: stoyo@chem.ous.ac.jp

0040–4020/01/$ - see front matter
PII: S0040-4020(01)00232-0

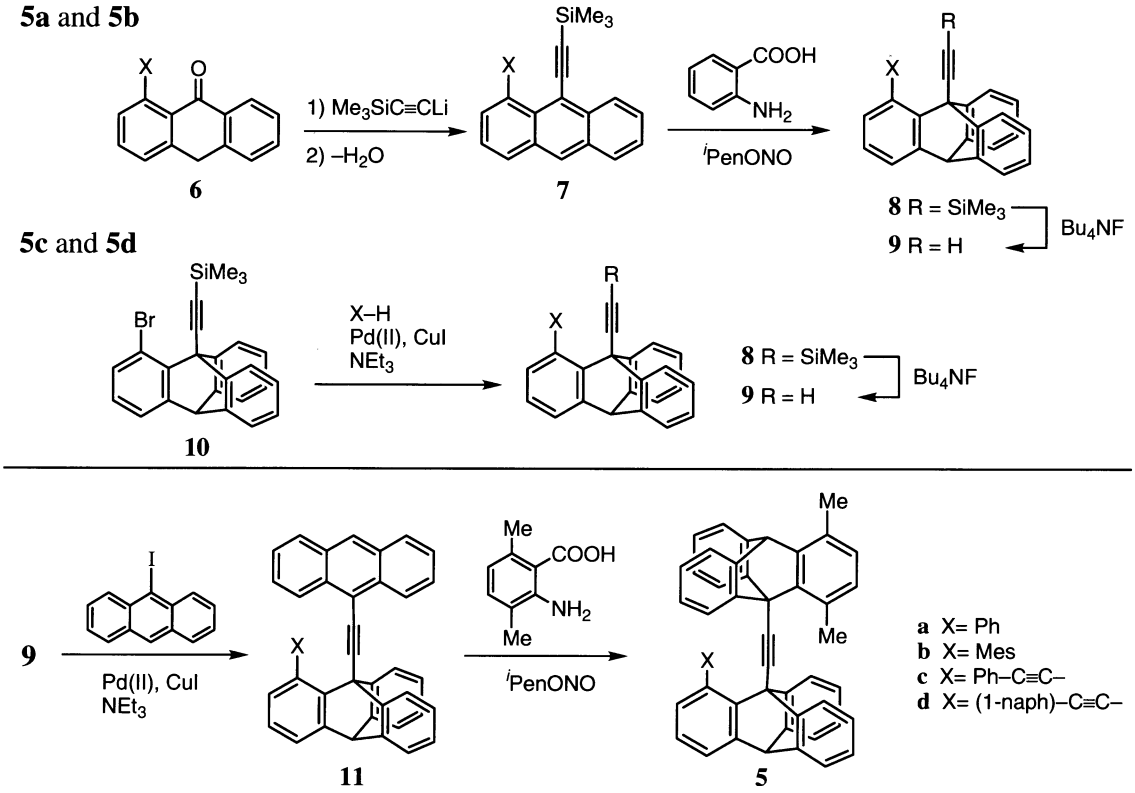

Scheme 2. Syntheses of (1,4-dimethyl-9-triptycyl)(1-substituted 9-triptycyl)ethynes (**5**).

those of **1**–**4** reported earlier (Scheme 2).[1,5] Aryl substituted compounds, **5a** and **b**, were synthesized from 1-aryl-9-anthrones, which were converted to 1-aryl-9-ethynyltriptycenes (**9**) in three steps. For **5c** and **d**, an arylethynyl group at the 1-position was introduced at the stage of the 1-bromo compound (**10**) by the Sonogashira reaction[7] with a terminal ethyne, and subsequent desilylation gave **9**. Thus the prepared 9-ethynyltriptycenes (**9**) were transformed to the desired compounds by the Sonogashira reaction with 9-iodoanthracene followed by the Diels–Alder reaction with 3,6-dimethylbenzyne.

Compounds **5a**–**d** exhibited two sets of ^{1}H NMR signals due to the *ap* and *sc* rotamers at room temperature. The assignment of the rotamer was apparent from the equivalency of the aromatic signals: the *sc* form gave a signal pattern more complicated than the *ap*. The spectra were measured at higher temperatures in 1,1,2,2-tetrachloroethane-d_2 to show lineshape changes due to the facile exchange between the two isomers. For example, the temperature dependence of the ^{1}H NMR signals of **5c** is shown in Fig. 1: the signals due to the 1-Me protons broaden at 70°C, and coalesce at 109°C. The total lineshape analysis of these signals afforded rates of interconversion between the *ap* and *sc* isomers via the bond rotation. The kinetic data are listed in Table 1 together with the free energy difference between the two rotamers (ΔG°), which was calculated from the rotamer population.

The molecular structures of **5** were obtained by X-ray analysis or MM2 calculation. Only the mesityl compound **5b** gave a single crystal suitable for X-ray analysis. An ORTEP drawing of **5b**, in which molecules take the *ap* conformation, is shown in Fig. 2 together with selected structural parameters. Molecular mechanics calculations were carried out for both the *ap* and *sc* forms of **5a**–**d** with the MM2 force-field parameters. The optimized

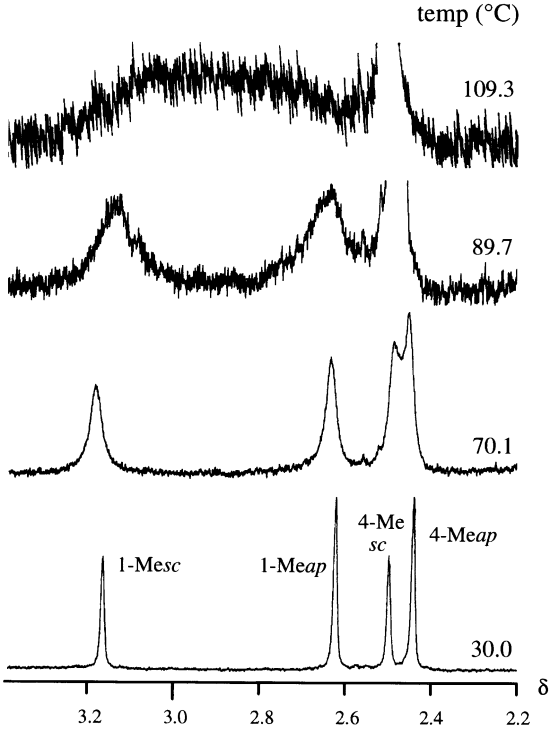

Figure 1. VT ^{1}H NMR spectra of Me signals in **5c** in 1,1,2,2-tetrachloroethane-d_2.

Table 1. Thermodynamic and kinetic parameters for rotation around C–C bonds (*ap*→*sc*) in compounds **5** in 1,1,2,2-tetrachloroethane-d_2

Compound	$\Delta H^{\neq}$ (kcal/mol)	$\Delta S^{\neq}$ (cal/(mol K))	$\Delta G^{\neq}_{273}$ (kcal/mol)	r^a (Å)	ΔG°_{273} (kcal/mol)
5a	14.7±0.4	−3.6±1.4	15.7	1.82	0.9
5b	19.8±0.4	3.4±1.0	18.8	2.13	2.4
5c	16.4±0.4	−3.8±1.0	17.5	2.00	0.7
5d	18.4±0.6	1.9±1.7	17.8	2.03	0.8

[a] Estimated steric size calculated by the linear relationship, r=0.102 $\Delta G^{\neq}_{273}$+0.22.[1]

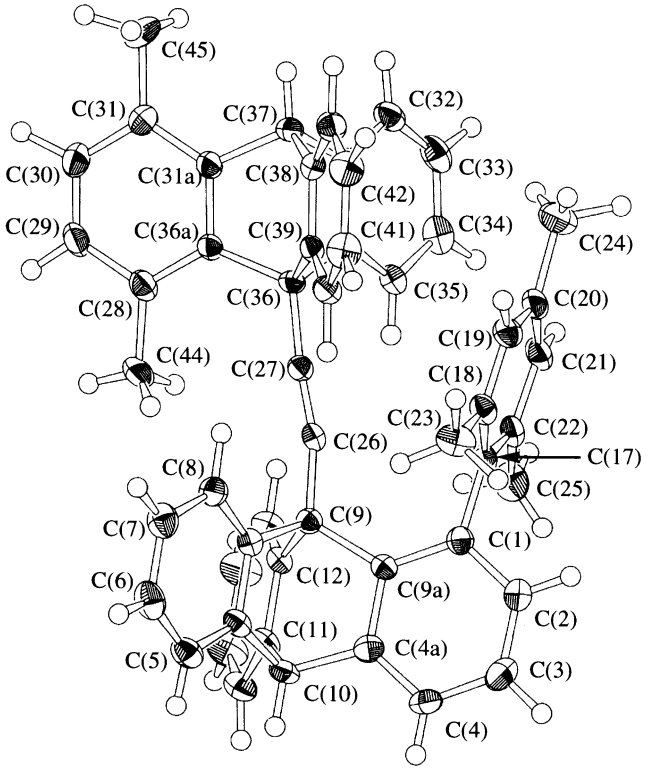

Figure 2. ORTEP drawing of compound **5b** with thermal ellipsoids at 50% probabilities (a solvent molecule is omitted for simplicity). Selected structural parameters: C(9)–C(26) 1.480(3), C(26)–C(27) 1.201(4), C(27)–C(36) 1.481(3) Å; C(9)–C(26)–C(27) 165.9(2)°, C(26)–C(27)–C(36) 172.1(3)°, C(9a)–C(1)–C(17) 124.8(2)°, C(9)–C(9a)–C(1) 129.1(2)°, C(26)–C(9)–C(9a) 119.2(2)°, C(9)–C(26)–C(27)–C(36) 133(1)°.

structures of *ap*-**5a** and *ap*-**5c** are shown in Fig. 3. The calculated bond angles of the acetylenic carbons are listed in Table 2 as a scale of the molecular strain together with the observed ^{13}C NMR chemical shifts.

3. Discussion

The free energies of activation for the C(sp)–C(sp^3) bond rotation increase in the order of **5a**<**5c**≈**5d**<**5b** from 15.7 to 18.8 kcal/mol. A comparison of these data with those of compounds **1**–**4** reveals that the steric effect of the 1′-substituent on the rotational barrier is increased in the order H<F<OMe<Cl<Me≈Ph<Br<I≈arylethynyl<Mes.

The effect of Ph is in the middle of Cl and Br, and comparable to Me. The arylethynyl groups are comparable to I in size. The highest barrier was observed for the Mes compound (**5b**) in the series of compounds, being the highest among the rotational barriers in acyclic acetylene compounds to the best of our knowledge.

For a quantitative estimation, the kinetic data of **5** are correlated with the linear relationship between the $\Delta G^{\neq}$ and r (van der Waals radius)[8] established for compounds **1**–**4**, $\Delta G^{\neq}_{273}$ (kcal/mol)=9.84r (Å)− 2.2 (Fig. 4).[1] The observed $\Delta G^{\neq}_{273}$ values of **5a**–**d** are input to the equation to afford the r values of 1.82, 2.13, 2.00 and 2.03 Å, respectively, which are regarded as 'estimated steric size' derived by the rotational barrier in the BTE system. The calculated r values indicate that arylethynyl groups are little larger than Ph, and mesityl group is larger by 0.3 Å than Ph. The steric size of Ph group determined by various methods is 1.62,[9] 1.77[8] and 1.77 Å,[10] and our estimation is consistent with the latter two cases. The value of ca. 1.8 Å corresponds to the thickness of π electron cloud of a benzene plane at each side.[8,11] Although examples are limited at present, the BTE system provides a useful method for the estimation of steric size of not only spherically but also nonspherically shaped substituents.

In the X-ray structure of *ap*-**5b**, several bending deformations due to the steric hindrance are notable, while the bond distances are generally in normal ranges. The mesityl group conformationally bisects the attaching benzeno plane, and tilts away from the acetylenic (1,4-Me$_2$-trip) moiety to a large extent to avoid the steric interactions with the 1,4-dimethyl-9-triptycyl group: the bond angles of C(26)–C(9)–C(9a), C(9)–C(9a)–C(1) and C(9a)–C(1)–C(17) are larger than standard values. Therefore, the distance between the mesityl group and acetylenic axis becomes large at the tip of the mesityl-phenyl group, C(20)···C(36) 4.23 Å, compared with that between the attached *peri* positions, C(1)···C(9) 2.68 Å.

Another structural feature is the bending deformation of the acetylenic moiety, the bond angles being 166° and 172° at C(26) and C(27), respectively. The former is one of the smallest angles for sp carbons among nonconjugated acyclic alkynes.[12] The bending deformation of acetylenic carbons usually results in the deshielding of carbon atoms in ^{13}C NMR spectroscopy due to the rehybridization.[13–15] In **5b**, only one of the two sp carbon signals is slightly shifted downfield relative to an unstrained compound, 2,2,5,5-tetrametheyl-3-hexyne, at δ 86.7 (Table 2).[16] In contrast, a notable shift down to δ 91–92 was observed for some signals in **5a**, **b**, and **c** (Table 2). We cannot rationalize why the effect of the bond strain on the ^{13}C NMR chemical shift is so small in **5b** from available information. However, the fact that the signals due to the sterically congested *sc* form are always at lower field by 0.4–1.2 ppm than those due to the *ap* in **5a**, **b**, and **c** is attributed to the effect of hybridization.

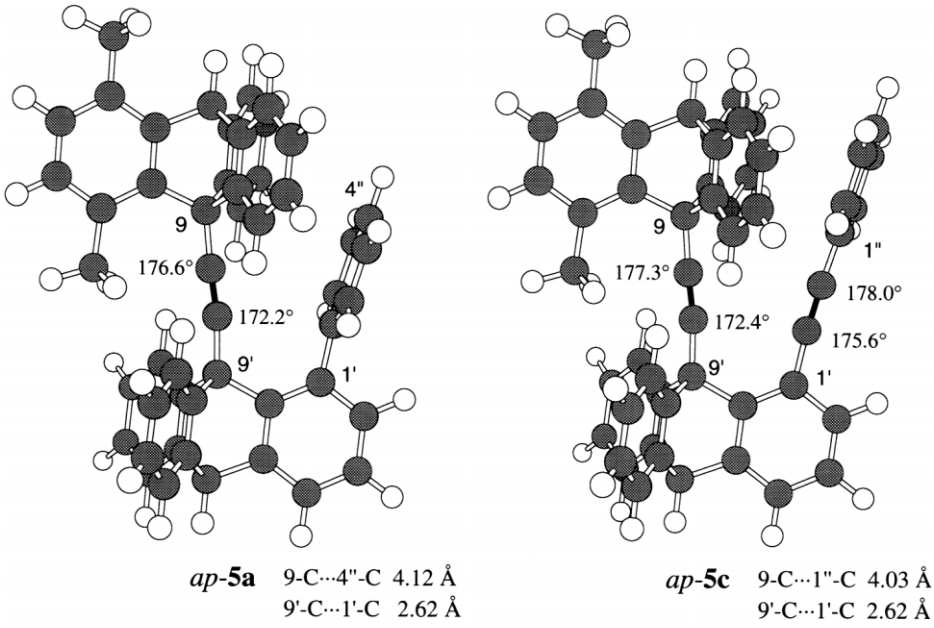

Figure 3. Optimized structures of *ap*-**5a** and *ap*-**5c** by MM2 calculations and selected structural parameters (triple bonds are indicated by solid cylinders).

Table 2. Bond angles and ^{13}C NMR data of acetylenic carbons in compounds **5** and the related compounds

Compound 1′-X	**5a** Ph	**5b** Mes	**5c** Ph–C≡C–	**5d** Naph–C≡C–	**1**[a] H	**3**[a] Me
Bond angle (°)[b]						
ap 1-C	176.7	177.4 (172.1)	177.3	177.2	173.8	175.6 (170.2)
ap 2-C	172.2	171.3 (165.9)	172.4	172.3	177.7	175.6 (171.4)
sc 1-C	173.3	173.0	173.0	172.3	–[c]	166.7
sc 2-C	171.3	170.4	172.8	172.9		166.7
^{13}C NMR (δ)[d]						
ap	88.20	87.32	87.34	87.29	87.83	89.40
ap	91.63	89.42	91.34	91.45	90.34	
sc	89.34	–[e]	87.76	87.75	–[c]	90.30
sc	92.79		92.10	92.19		

[a] Ref. 1.
[b] 1-C and 2-C denote the sp carbons attaching to 1,4-Me_2-trip and 1-X-trip groups, respectively. Values in parentheses are experimental values determined by X-ray analysis.
[c] Identical with *ap*.
[d] Solvent $CDCl_3$. Measured at room temperature except for **2** (−50°C), cf. δ 86.7 (^{t}Bu–C≡C–^{t}Bu).[16]

As shown by the structural data of **5b** as well as **3** in Table 2, the MM2 calculation tends to underestimate the bending formations of the acetylenic carbons. Nevertheless, the calculated bond angles are helpful to know the molecular strain in the initial state of the dynamic process. Although the barrier in **5b** is higher by 3.0 kcal/mol than that in **5a**, the calculated bond angles in the two compounds are not so different from each other. This suggests that the steric effect in the transition state rather than the initial state plays a dominant role in controlling the barrier heights. The high barrier in **5b** is attributed to the direct steric interactions of three extra Me groups with the 1,4-Me_2-trip group that passes over the 1′-substituent at the transition state. Additionally, the conformational rigidity of the mesityl group due to the steric effect of the 2,6-Me_2 groups makes it difficult to avoid the steric interactions during the rotation around the acetylenic axis.

We anticipated that arylethynyl groups should be effective to enhance the rotational barrier because they were large enough to reach a notch between two benzeno groups in the 1,4-Me_2-trip moiety in a rigid molecular model. In fact, there are some short contacts (3.1–3.3 Å for C···C distances)[17] between the phenyl group in the 1′-substituent and the nonsubstituted benzeno groups in 1,4-Me_2-trip group in the calculated structure of *ap*-**5c**. However, severe steric congestion is reduced by the bending deformations of the two C–C≡C–C moieties: the interatomic distance of 9-C···1″-C is much longer than that between the *peri* positions (Fig. 3). Although information about the structure in the transition state is limited, its energy level is not raised so much because of the flexibility of the substituents to reduce severe steric interactions. As a result, the phenylethynyl group has a moderate effect on the barrier enhancement. The substitution of a 1-naphthyl group for the phenyl group in **5c** hardly influences the rotational barrier because the additionally fused benzene ring is far from the site where the bond rotation occurs.

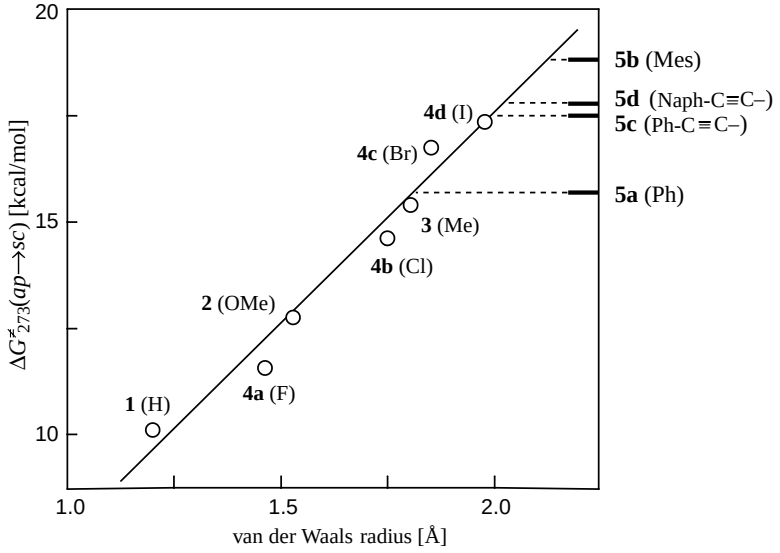

Figure 4. Plot of vd*W* radius of 1′-substituents vs $\Delta G^{\neq}$ for compounds **1**–**5**.

In summary, the barrier to rotation around C(sp)–C(sp^3) bond is enhanced in the order of the phenyl, arylethynyl and mesityl substituted compounds in the BTE system. The kinetic and structural data indicate that not only the steric bulkiness but also the shape and flexibility of the substituents are important factors in determining the barrier heights. Especially, the springy nature of the C–C≡C–C moieties is efficient to relieve the excess steric strain in the transition state as well as in the initial state in these sterically crowded compounds. The introduction of a mesityl group is not sufficient to interlock the two 9-triptycyl groups across the acetylenic axis on a laboratory time scale. It is necessary to introduce bulky and rigid substituents at more than two *peri* positions toward successful isolation of this kind of rotational isomer.

4. Experimental

4.1. General

^{1}H and ^{13}C NMR spectra were measured on a Varian Gemini-300 at 300 and 75 MHz, respectively. The spectra were collected at room temperature unless otherwise mentioned. Melting points are uncorrected. Elemental analyses were performed on a Perkin–Elmer 2400 series analyzer. High-resolution mass spectra were measured on a JEOL JMS-700 MStation spectrometer. 1-Mesityl-9-anthrone was prepared by the Suzuki coupling[18] of 1-iodoanthraquinone[19] with mesitylboronic acid, followed by reduction with Sn/HCl:[20] ^{1}H NMR ($CDCl_3$) δ 1.87 (s, 6H), 2.37 (s, 3H), 4.55 (s, 2H), 6.96 (s, 2H), 7.10 (d, *J*=8.6 Hz, 1H), 7.38 (t, *J*=8.1 Hz, 1H), 7.46 (d, *J*=7.8 Hz, 1H), 7.51 (dt, *J*=1.1, 7.7 Hz, 1H), 7.57 (dd, *J*=1.5, 7.8 Hz, 1H), 7.61 (t, *J*=7.6 Hz, 1H), 8.15 (dd, *J*=1.3, 8.0 Hz, 1H).

4.1.1. 1-Phenyl-9-[(trimethylsilyl)ethynyl]anthrancene (7a). This compound was similarly prepared from 3.7 mmol of lithium (trimethylsilyl)acetylide and 500 mg (1.85 mmol) of 1-phenyl-9-anthrone[21] in ether by the method described in the literature.[1,5] The crude material was subjected to chromatography on silica gel with hexane eluent, during which the initially formed 1-phenyl-9-[(trimethylsilyl)ethynyl]-9-anthrol was dehydrolyzed into the corresponding anthracene. The desired compound was obtained as yellow oil, which crystallized upon standing, with the recovery of 137 mg of the starting anthrone. Yield 307 mg (47%). Mp 98–101°C; ^{1}H NMR ($CDCl_3$) δ 0.09 (s, 9H), 7.34–7.58 (m, 9H), 7.97–8.03 (m, 2H), 8.49 (s, 1H), 8.55 (d, *J*=8.7 Hz, 1H). Anal. calcd for $C_{25}H_{22}Si$: C, 85.66; H, 6.33. Found: C, 85.38; H, 6.41.

4.1.2. 1-Mesityl-9-[(trimethylsilyl)ethynyl]anthrancene (7b). Yield 53%. Yellow oil; ^{1}H NMR ($CDCl_3$) δ 0.15 (s, 9H), 1.89 (s, 6H), 2.40 (s, 3H), 6.90 (s, 2H), 7.19 (dd, *J*=1.4, 6.8 Hz, 1H), 7.47–7.52 (m, 2H), 7.56 (dt, *J*=1.5, 6.5 Hz, 1H), 8.00 (d, *J*=8.6 Hz, 2H), 8.49 (s, 1H), 8.45 (dd, *J*=1.2, 8.3 Hz, 1H); HRMS (FAB) Found: MH^+ 393.2016. Calcd for $C_{28}H_{28}{}^{28}Si$: 393.2039.

4.1.3. 1-Phenyl-9-[(trimethylsilyl)ethynyl]triptycene (8a). This compound was similarly prepared by the Diels–Alder reaction of **7a** with 3 equiv. of benzyne as the method in the literature.[1,5] Yield 57%. Mp 228–230°C (recrystallized from hexane); ^{1}H NMR ($CDCl_3$) δ 0.12 (s, 9H), 5.43 (s, 1H), 6.78 (dd, *J*=1.4, 7.7 Hz, 1H), 6.97 (t, *J*=7.5 Hz, 1H), 7.02–7.12 (m, 4H), 7.24 (dd, *J*=1.4, 7.9 Hz, 2H), 7.30–7.43 (m, 6H), 7.72 (m, 2H). Anal. calcd for $C_{31}H_{26}Si$: C, 87.27; H, 6.14. Found: C, 86.96; H, 6.19.

4.1.4. 1-Mesityl-9-[(trimethylsilyl)ethynyl]triptycene (8b). Yield 63%. Mp 201–202°C; ^{1}H NMR ($CDCl_3$) δ 0.14 (s, 9H), 1.72 (s, 6H), 2.38 (s, 3H), 5.42 (s, 1H), 6.57 (dd, *J*=1.3, 7.7 Hz, 1H), 6.85 (s, 2H), 6.99 (t, *J*=7.5 Hz, 1H), 7.04–7.08 (m, 4H), 7.34 (dd, *J*=1.4, 7.3 Hz, 1H), 7.38–7.42 (m, 2H), 7.64–7.70 (m, 2H). Anal. calcd for $C_{34}H_{32}Si$: C, 87.13; H, 6.88. Found: C, 87.12; H, 6.90.

4.1.5. 9-Ethynyl-1-phenyltriptycene (9a). 8a was desilylated by treatment with Bu_4NF in THF in the usual manner.[1,5] Yield 79%. Mp 171–172°C (recrystallized from hexane); ^{1}H NMR ($CDCl_3$) δ 2.50 (s, 1H), 5.45 (s, 1H), 6.84 (dd, *J*=1.3,

7.7 Hz, 1H), 7.00 (t, *J*=7.3 Hz, 1H), 7.03–7.10 (m, 2H), 7.23 (dd, *J*=1.6, 8.3 Hz, 2H), 7.32 (t, *J*=6.8 Hz, 2H), 7.35–7.44 (m, 6H), 7.71 (m, 2H). Anal. calcd for $C_{28}H_{18}$: C, 94.88; H, 5.12. Found: C, 94.86; H, 5.11.

4.1.6. 9-Ethynyl-1-mesityltriptycene (9b). Yield 73%. Mp 184–185°C (recrystallized from hexane–dichloromethane); ^{1}H NMR ($CDCl_3$) δ 1.73 (s, 6H), 2.34 (s, 1H), 2.39 (s, 3H), 5.43 (s, 1H), 6.67 (dd, *J*=1.6, 7.7 Hz, 1H), 6.86 (s, 2H), 7.00–7.08 (m, 5H), 7.37 (dd, *J*=1.3, 7.3 Hz, 1H), 7.39–7.43 (m, 2H), 7.64–7.70 (m, 2H). Anal. calcd for $C_{31}H_{24}$: C, 93.90; H, 6.10. Found: C, 93.71; H, 6.07.

4.1.7. 9-Ethynyl-1-(phenylethynyl)triptycene (9c). To a solution of 995 mg (2.32 mmol) of 1-bromo-9-[(trimethylsilyl)ethynyl]triptycene (**10**)[1] and 1.55 ml (14.1 mmol) of phenylacetylene in 50 ml of degassed NEt_3 were added 98 mg (0.14 mmol) of $[PdCl_2(PPh_3)_2]$ and 14 mg (0.073 mmol) of CuI under nitrogen atmosphere. The solution was heated at 60°C for 27 h. After the solvent was evaporated, the residue was subjected to chromatography on silica gel with hexane–dichloromethane (20:1) eluent to give a mixture of the cross-coupling product and its desilylated compound in ca. 1:2 ratio. The analytical sample of the former was obtained by chromatography on silica gel as colorless oil. 1-Phenylethenyl-9-[(trimethylsilyl)ethynyl]triptycene (**8c**): ^{1}H NMR ($CDCl_3$) δ 0.12 (s, 9H), 5.36 (s, 1H), 6.95 (t, *J*=7.3 Hz, 1H), 7.05 (dt, *J*=1.2, 7.3 Hz, 2H), 7.11 (dt, *J*=1.2, 7.3 Hz, 2H), 7.19 (dd, *J*=1.2, 7.3 Hz, 2H), 7.32 (dd, *J*=1.2, 7.3 Hz, 1H), 7.33–7.40 (m, 5H), 7.58 (dd, *J*=1.5, 7.9 Hz, 2H), 7.89 (d, *J*=7.3 Hz, 2H); HRMS (FAB) Found: MH^+ 451.1771. Calcd for $C_{33}H_{26}{}^{28}Si$: 451.1782. The above mixture was completely desilylated by treatment with fluoride in a similar manner. Overall yield 67%. Colorless oil; ^{1}H NMR ($CDCl_3$) δ 3.27 (s, 1H), 5.39 (s, 1H), 6.98 (t, *J*=7.6 Hz, 1H), 7.06 (dt, *J*=1.5, 7.3 Hz, 2H), 7.11 (dt, *J*=1.5, 7.2 Hz, 2H), 7.21 (dd, *J*=1.5, 7.8 Hz, 1H), 7.34 (dd, *J*=1.3, 7.3 Hz, 1H), 7.38–7.43 (m, 5H), 7.59 (dd, *J*=1.7, 7.3 Hz, 2H), 7.92 (dd, *J*=1.7, 7.0 Hz, 2H); HRMS (EI) Found: M^+ 392.1937. Calcd for $C_{28}H_{28}{}^{28}Si$: 392.1960.

4.1.8. 9-Ethynyl-1-[(1-naphtyl)ethynyl]triptycene (9d). This compound was similarly prepared from **10** and 1-ethynylnaphthalene by Sonogashira coupling followed by desilylation. 1-[(1-Naphthyl)ethynyl]-9-[(trimethylsilyl)-ethynyl]triptycene (**8d**): colorless oil; ^{1}H NMR ($CDCl_3$) δ −0.16 (s, 9H), 5.42 (s, 1H), 7.01 (t, *J*=7.6 Hz, 1H), 7.09 (dt, *J*=1.3, 7.0 Hz, 2H), 7.15 (dt, *J*=1.5, 7.5 Hz, 2H), 7.31 (dd, *J*=1.5, 8.0 Hz, 1H), 7.37 (dd, *J*=1.4, 7.3 Hz, 1H), 7.42 (dd, *J*=1.5, 7.7 Hz, 2H), 7.50 (t, *J*=8.2 Hz, 1H), 7.55 (dt, *J*=1.6, 7.1 Hz, 1H), 7.61 (dt, *J*=2.1, 8.0 Hz, 1H), 7.82 (dd, *J*=1.2, 7.2 Hz, 1H), 7.86 (d, *J*=7.1 Hz, 1H), 7.89 (d, *J*=7.9 Hz, 1H), 7.93 (d, *J*=7.4 Hz, 2H), 8.55 (d, *J*=8.2 Hz, 1H); HRMS (FAB) Found: MH^+ 501.2044. Calcd for $C_{37}H_{28}{}^{28}Si$: 501.2039. The terminal acetylene was purified by chromatography on silica gel. Overall yield 84%. Colorless oil; ^{1}H NMR ($CDCl_3$) δ 3.13 (s, 1H), 5.42 (s, 1H), 7.03 (t, *J*=7.6 Hz, 1H), 7.08 (dt, *J*=1.4, 6.7 Hz, 2H), 7.13 (dt, *J*=1.5, 7.0 Hz, 2H), 7.34 (dd, *J*=1.6, 7.8 Hz, 1H), 7.38 (d, *J*=8.5 Hz, 1H), 7.41 (dd, *J*=1.4, 6.7 Hz, 2H), 7.51 (t, *J*=7.8 Hz, 1H), 7.55 (dt, *J*=1.2, 6.7 Hz, 1H), 7.61 (dt, *J*=1.4, 6.7 Hz, 1H), 7.82 (dd, *J*=1.2, 6.0 Hz, 1H), 7.87 (d, *J*=6.8 Hz, 1H), 7.89 (d, *J*=9.4 Hz, 1H), 7.94 (dd, *J*=1.7, 7.0 Hz, 2H), 8.54 (d, *J*=8.1 Hz, 1H); HRMS (FAB) Found: MH^+ 429.1660. Calcd for $C_{34}H_{20}$: 429.1643.

4.1.9. 9-[(9-Anthryl)ethynyl]-1-phenyltriptycene (11a). This compound was similarly prepared from 100 mg (0.282 mmol) of **9a**, 120 mg (0.394 mmol) of 9-iodoanthracene,[22] 28 mg (0.040 mmol) of $[PdCl_2(PPh_3)_2]$ and 3.8 mg (0.020 mmol) of CuI by the literature method.[1,5] The crude materials were chromatographed on silica gel with hexane–dichloromethane eluent. The order of elution was 9-iodoanthracene, the starting compound, the coupling product and a by-product (homo coupling product). The third fraction was collected and recrystallized from hexane–dichloromethane to give 65 mg (43%) of the desired compound as yellow crystals containing solvent molecules. Mp 259–262°C; ^{1}H NMR ($CDCl_3$) δ 5.56 (s, 1H), 6.17 (t, *J*=7.4 Hz, 1H), 6.63 (t, *J*=7.5 Hz, 2H), 6.86 (dd, *J*=1.3, 7.7 Hz, 1H), 7.06 (t, *J*=7.5 Hz, 1H), 7.10–7.20 (m, 4H), 7.28 (dd, *J*=1.2, 8.2 Hz, 2H), 7.45–7.58 (m, 8H), 8.02 (d, *J*=7.2 Hz, 2H), 8.13 (d, *J*=6.8 Hz, 2H), 8.42 (s, 1H), 8.46 (d, *J*=6.8 Hz, 2H). Anal. calcd for $C_{42}H_{26}\cdot 1/8(CH_2Cl_2)$: C, 93.47; H, 4.89. Found: C, 93.14; H, 4.82. MS (FAB) Found: MH^+ 531. Calcd for $C_{42}H_{26}$: 531.

4.1.10. 9-[(9-Anthryl)ethynyl]-1-mesityltriptycene (11b). Yield 65%. Yellow powder; mp 247–254°C (dec); ^{1}H NMR ($CDCl_3$) δ 0.71 (s, 3H), 1.84 (s, 6H), 5.54 (s, 1H), 5.98 (s, 2H), 6.67 (dd, *J*=1.3, 7.7 Hz, 1H), 7.08 (t, *J*=7.5 Hz, 1H), 7.11 (dt, *J*=1.8, 6.7 Hz, 2H), 7.17 (dt, *J*=1.5, 7.5 Hz, 2H), 7.46 (dd, *J*=1.3, 8.3 Hz, 1H), 7.49 (dd, *J*=1.1, 7.2 Hz, 2H), 7.57 (dt, *J*=1.3, 6.7 Hz, 2H), 7.66 (dt, *J*=1.4, 7.7 Hz, 2H), 8.06 (d, *J*=8.1 Hz, 2H), 8.14 (dd, *J*=1.5, 7.1 Hz, 2H), 8.39 (s, 1H), 8.65 (d, *J*=8.7 Hz, 2H). Anal. calcd for $C_{45}H_{32}$: C, 94.37; H, 5.63. Found: C, 94.23; H, 5.80.

4.1.11. 9-[(9-Anthryl)ethynyl]-1-(phenylethynyl)triptycene (11c). Yield 62%. Yellow crystals; mp 258–269°C (dec); ^{1}H NMR ($CDCl_3$) δ 5.50 (s, 1H), 6.36 (t, *J*=7.4 Hz, 2H), 6.45 (dd, *J*=1.5, 8.3 Hz, 2H), 7.03 (t, *J*=7.5 Hz, 1H), 7.13 (dt, *J*=1.4, 7.3 Hz, 2H), 7.21 (dt, *J*=1.4, 7.4 Hz, 2H), 7.23 (d, *J*=7.3 Hz, 1H), 7.42 (dd, *J*=1.4, 7.2 Hz, 1H), 7.46–7.49 (m, 5H), 7.57 (ddd, *J*=1.4, 6.6, 8.8 Hz, 2H), 7.93 (d, *J*=8.2 Hz, 2H), 8.28 (d, *J*=6.6 Hz, 2H), 8.31 (s, 1H), 9.03 (d, *J*=8.9 Hz, 2H). Anal. calcd for $C_{44}H_{26}$: C, 95.28; H, 4.72. Found: C, 95.15; H, 4.59.

4.1.12. 9-[(9-Anthryl)ethynyl]-1-[(1-naphtyl)ethynyl]-triptycene (11d). Yield 74%. Yellow crystals; mp 231–237°C (dec); ^{1}H NMR ($CDCl_3$) δ 5.53 (s, 1H), 6.42 (t, *J*=7.8 Hz, 1H), 6.59 (d, *J*=7.1 Hz, 1H), 6.93 (dd, *J*=1.3, 7.7 Hz, 1H), 7.04–7.23 (m, 7H), 7.29 (d, *J*=7.9 Hz, 1H), 7.33–7.42 (m, 5H), 7.46 (dd, *J*=1.1, 8.2 Hz, 1H), 7.51 (d, *J*=6.6 Hz, 2H), 7.71 (d, *J*=8.3 Hz, 2H), 7.94 (d, *J*=8.3 Hz, 1H), 7.98 (s, 1H), 8.32 (2H, d, *J*=7.1 Hz), 8.90 (d, *J*=8.8 Hz, 2H); HRMS (FAB) Found: MH^+ 605.2250. Calcd for $C_{48}H_{28}$: 605.2269.

4.1.13. (1,4-Dimethyl-9-triptycyl)(1-phenyl-9-triptycyl)-ethyne (5a). A solution of 65 mg (0.12 mmol) of **11a** in 10 ml of 1,2-dimethoxyethane (DME) was refluxed in a flask. From respective dropping funnels, a solution of 99 mg (0.60 mmol) of 3,6-dimethylanthranilic acid[23] in 5 ml of DME and a solution of 120 μl (0.90 mmol) of

isopentyl nitrite in 5 ml of DME were added to the boiling solution over 1 h. After the reaction mixture was refluxed for 2 h, the volatile materials were evaporated. The residue was passed through a plug silica gel column to remove polar materials, and the crude mixture was further chromatographed on silica gel with hexane–dichloromethane (1:1) eluent. Recrystallization from dichloromethane gave 42 mg (55%) of the product as colorless crystals. Mp 300–307°C (dec); ^{1}H NMR ($CDCl_3$) δ 2.33 (s, 3H*ap*), 2.45 (s, 3H*ap*), 2.50 (s, 3H*sc*), 2.65 (s, 3H*sc*), 5.55 (s, 1H), 5.60 (s, 1H*ap*), 5.60 (s, 1H*sc*), 6.13 (t, J=7.4 Hz, 1H*ap*), 6.43–7.88 (brm, 23H*ap*+26H*sc*), 8.20 (d, J=6.7 Hz, 2H*ap*), rotamer ratio (*ap*/*sc*) 62:38; ^{13}C NMR ($CDCl_3$) δ 18.87, 21.63, 21.84, 49.87, 53.84, 54.59, 54.58, 88.20, 89.34, 91.63, 92.79, and 58 aromatic carbon signals at 122.7–146.3. Anal. calcd for $C_{50}H_{34}$: C, 94.60; H, 5.40. Found: C, 94.69; H, 5.57.

4.1.14. (1,4-Dimethyl-9-triptycyl)(1-mesityl-9-triptycyl)-ethyne (5b). Yield 80%. Colorless crystals; mp 265–274°C (dec); ^{1}H NMR ($CDCl_3$) *ap* form δ 0.91 (s, 3H), 1.92 (s, 6H), 2.24 (s, 3H), 2.44 (s, 3H), 5.54 (s, 1H), 5.61 (s, 1H), 6.14 (s, 2H), 6.41 and 6.61 (ABq, J=7.8 Hz, 2H), 6.63 (dd, J=1.4, 7.7 Hz, 1H), 7.03–7.24 (m, 9H), 7.39 (d, J=7.0 Hz, 2H), 7.43 (d, J=7.2 Hz, 1H), 7.52 (dd, J=1.6, 6.8 Hz, 2H), 7.81 (d, J=7.2 Hz, 2H), 8.16 (d, J=7.1 Hz, 2H); *sc* form (readable signals only) δ 1.78 (s, 3H), 1.90 (s, 3H), 1.98 (s, 3H), 2.84 (s, 3H), 2.50 (s, 3H), rotamer ratio (*ap*/*sc*) 97:3; ^{13}C NMR ($CDCl_3$) δ 18.88, 19.24, 21.42, 21.80, 49.88, 53.54, 54.07, 54.50, 87.32, 89.42, and 28 aromatic carbon signals 122.50–146.17; HRMS (FAB) Found: MH^+ 677.3236. Calcd for $C_{53}H_{40}$: 677.3208.

4.1.15. (1,4-Dimethyl-9-triptycyl)[1-(phenylethynyl)-9-triptycyl]ethyne (5c). Yield 24%. Colorless crystals; mp 323–351°C (dec); ^{1}H NMR ($CDCl_3$) δ 2.48 (s, 3H*ap*), 2.54 (s, 3H*sc*), 2.65 (s, 3H*ap*), 3.22 (s, 3H*sc*), 5.51 (s, 1H), 5.60 (s, 1H*ap*), 5.69 (s, 1H*sc*), 5.93 (d, J=7.7 Hz, 2H*ap*), 6.46–7.52 (m, 22H*ap*+24H*sc*), 7.80–7.88 (m, 2H*sc*), 8.30–8.39 (m, 2H*ap*+1H*sc*), 8.43 (d, J=7.1 Hz, 2H*ap*), 8.54 (d, J=7.2 Hz, 1H*sc*), rotamer ratio (*ap*/*sc*) 44:56; ^{13}C NMR ($CDCl_3$) δ 18.88, 22.03, 22.10, 49.88, 49.99, 53.62, 53.86, 54.07, 87.34, 87.76, 88.09, 89.00, 91.34, 92.11, 96.56, 96.56, and 50 aromatic carbon signals at 119.7–146.1. Anal. calcd for $C_{52}H_{34}$·1/4(CH_2Cl_2): to C, 92.28; H, 5.11. Found: C, 92.24; H, 5.12. HRMS (FAB) Found: MH^+ 659.2728. Calcd for $C_{52}H_{34}$: 659.2739.

4.1.16. (1,4-Dimethyl-9-triptycyl){1-[(1-naphthyl)ethynyl]-9-triptycyl}ethyne (5d). Yield 54%. Colorless crystals; mp 304–322°C (dec); ^{1}H NMR ($CDCl_3$) δ 2.45 (s, 3H*ap*), 2.53 (s, 3H*sc*), 2.64 (s, 3H*ap*), 3.15 (s, 3H*sc*), 5.15 (d, J=7.1 Hz, 1H*ap*), 5.54 (s, 1H), 5.56 (s, 1H*ap*), 5.67 (s, 1H*sc*), 6.09–7.68 (m, 22H*ap*+24H*sc*), 7.79–7.88 (m, 2H*sc*), 8.08 (d, J=6.8 Hz, 1H*ap*), 8.29–8.40 (m, 4H*ap*+1H*sc*), 8.47 (d, J=7.1 Hz, 1H*sc*), rotamer ratio (*ap*/*sc*) 49:51; ^{13}C NMR ($CDCl_3$) δ 18.86, 22.10, 49.83, 49.96, 53.61, 53.92, 54.08, 87.29, 87.75, 91.45, 92.19, 93.18, 93.98, 94.75, and 55 aromatic carbon signals at 119.8–146.2. Anal. calcd for $C_{56}H_{36}$: C, 94.88; H, 5.12. Found: C, 94.59; H, 5.33.

4.2. X-Ray analysis

A crystal of **5b** used for the measurement was grown from a hexane–chloroform solution. The crystal size was 0.20×0.20×0.10 mm^3. The diffraction data were collected on a Rigaku RAXIS-IV imaging plate diffractometer with MoKα radiation (λ=0.71070 Å) to a maximum 2θ value of 55.1° at −80°C. A total of 12×6.00° oscillation images were collected, each being exposed for 90.0 min. The reflection data were corrected for the Lorentz-polarization effects and secondary extinction (coefficient=3.65472×10^{-6}). The crystal-to-detector distance was 100.0 mm with the detector at the zero swing position. The readout was performed in the 0.100 mm pixel mode. The structure was solved by the direct method and refined by the full-matrix least-squares method by using a TEXSAN program on a Comtec O2 workstation. The non-hydrogen atoms were refined anisotropically. Some hydrogen atoms were refined isotropically, and the rest were included in fixed positions. Among 8439 observed reflections, 6362 reflections ($I>3.0\sigma(I)$) were used for the refinement of 671 variables. The function minimized was $\sum[w(|F_o| - |F_c|)^2]$, where $w = [\sigma_c^2|F_o| + (p^2/4)|F_o|^2]^{-1}$ (p=0.1610). Formula $C_{53}H_{40}$·$CHCl_3$, FW 796.28, monoclinic, space group $P2_1/n$, a=22.0004(2), b=8.299(2), c=24.133(3) Å, β=111.849(7)°, V=4090.4(9) Å^3, Z=4, D_c=1.293 g/cm^3, μ(MoKα)=2.62 cm^{-1}, R=0.080, R_w=0.148, goodness of fit 1.82. Additional information will be given from CCDC.

4.3. MM calculation

The calculations were carried out by the CHEM3D Pro ver. 5.0 program.[24] The MM2 force-field parameters were employed without modification.

4.4. Dynamic NMR measurement

Variable temperature ^{1}H NMR spectra were measured on a Bruker AMX-400 at 400 MHz. About 5 mg of sample was dissolved in ca. 0.6 ml of 1,1,2,2-tetrachloroethane-d_2. During VT measurements, the temperatures of the sample were read from a thermocouple equipped with the instrument after calibration with the chemical shift differences of the methanol or 1,2-ethanediol signals. The total lineshape analysis was performed by the DNMR3K program, which is a modified version of the DNMR3 program.[25] Lineshapes of the 1-Me signals were analyzed as exchange between two unpopulated sites. Chemical shift differences and rotamer populations were measured at several temperatures where the rotation takes place very slowly on the NMR time scale. The chemical shift differences ($\Delta\nu$) were assumed to be correlated linearly with the temperature (t, °C). The rotamer population was analyzed by the van't Hoff equation. Spin–spin relaxation times (T_2) were estimated from the lineshapes at slow exchange limit. Selected input parameters and rate constants ($k_{ap\rightarrow sc}$) are as follows. **5a**: $\Delta\nu$=0.738t+45.1 Hz, T_2=0.07–0.09 s; k, s^{-1} [t, °C]=16.0 [24.8], 28.0 [31.0], 46 [37.1], 74 [43.3], 120 [49.4], 180 [55.6]. **5b**: $\Delta\nu$=0.145t+150.5 Hz, T_2=0.12–0.15 s; k, s^{-1} [t, °C]=7.0 [65.9], 11.0 [71.0], 17.0 [76.1], 26.0 [81.2], 40 [86.2], 62 [91.4], 89 [96.5], 125 [101.4], 180 [106.8]. **5c**: $\Delta\nu$=0.072t+215.0 Hz, T_2=0.09–0.10 s; k, s^{-1} [t, °C]=36.0 [70.1], 55 [75.0], 73 [79.9], 100 [84.8], 140 [89.7], 190

[94.6], 270 [99.5], 360 [104.4], 480 [109.3], 650 [114.2]. **5d**: $\Delta\nu=0.031t+189.0$ Hz, $T_2=0.10$–0.11 s; k, s^{-1} [t, °C]=16.5 [60.8], 26.0 [65.7], 40 [71.0], 62 [75.9], 95 [81.1], 143 [86.2], 205 [91.4], 270 [96.2], 380 [101.6], 530 [106.5].

Acknowledgements

The present work was partly supported by a special fund from the Japan Private School Promotion Foundation. The helpful discussion of Prof. M. Ōki is greatly appreciated. The authors also thank Dr H. Akashi for his assistance with X-ray data analysis.

References

1. Part 3 of the series 'Rotational Isomerism Involving an Acetylenic Carbon.' Part 2: Toyota, S.; Yamamori, T.; Makino, T.; Ōki, M. *Bull. Chem. Soc. Jpn* **2000**, *73*, 2591–2597.
2. Eliel, E.; Wilen, S. H.; Mander, L. N. *Stereochemistry of Organic Compounds*; Wiley: New York, 1993 (Chapter 10).
3. The upper limit of the barrier to rotation around the C(sp)–C(sp^3) bonds in 2-butyne is 4 cm^{-1} (10 cal/mol): Olson, W. B.; Papousek, D. *J. Mol. Spectrosc.* **1971**, *37*, 527–534.
4. Koo Tze Mew, P.; Vögtle, F. *Angew. Chem., Int. Ed. Engl.* **1979**, *18*, 159–161.
5. Toyota, S.; Yamamori, T.; Asakura, M.; Ōki, M. *Bull. Chem. Soc. Jpn* **2000**, *73*, 205–213.
6. *Dynamic Nuclear Magnetic Resonance Spectroscopy*; Jackman, L. M., Cotton, F. A., Eds.; Academic: New York, 1975. Ōki, M. *Applications of Dynamic NMR Spectroscopy to Organic Chemistry*; VCH: Deerfield Beach, 1985.
7. Takahashi, S.; Kuroyama, Y.; Sonogashira, K.; Hagihara, N. *Synthesis* **1980**, 627–630.
8. Bondi, A. *J. Phys. Chem.* **1964**, *68*, 441–451.
9. Bott, G.; Field, D. L.; Sternhell, S. *J. Am. Chem. Soc.* **1980**, *102*, 5618–5626.
10. Charton, M. *J. Org. Chem.* **1976**, *41*, 2217–2220 (and references therein).
11. Nishio, M.; Hirota, M.; Umezawa, Y. *The CH/π Interaction*; Wiley-VCH: New York, 1998 (Chapter 3). Deakyne, C. A. In *Molecular Interactions*; Scheiner, S., Ed.; Wiley: Chichester, 1997 (Chapter 4).
12. The Cambridge Crystallographic Database analysis was performed for nonconjugated acyclic alkynes with the substructure of C(sp^3)–C(sp)≡C(sp)–C(sp^3) to give 14 structures in which at least one bond angle was smaller than 174°. Twenty of these structures carry functional groups such as –OH, $-NR_3^+$ at the α-position (169.9–173.2°). As for alkynes without α-functional groups, the values of 172.2° and 172.6° were found in a sterically crowded tricyclic compound and a simple alkynoic acid, respectively. The bond angle observed in *ap*-**3** (170.2°),[5] which has not registered in the database yet, is smaller than these angles.
13. Breitmaier, E.; Voelter, W. *Carbon-13 NMR Spectroscopy*; VCH: New York, 1990 (Chapter 4.3).
14. Meier, H.; Petersen, H.; Kolshorn, H. *Chem. Ber.* **1980**, *113*, 2398–2409.
15. For recent examples of strained cyclic acetylenes and their ^{13}C NMR, see: Kawase, T.; Ueda, N.; Darabi, H. R.; Oda, M. *Angew. Chem., Int. Ed. Engl.* **1996**, *35*, 1556–1558. Leung, C.-Y.; Mak, T. C. W.; Wong, H. N. C. *J. Chem. Crystallogr.* **1996**, *26*, 227–230. Tykwinski, R. R. *Chem. Commun.* **1999**, 905–906. Haberhauser, G.; Rominger, F.; Gleiter, R. *J. Chem. Soc., Perkin Trans. 2* **1999**, 947–950.
16. Dubois, J.-E.; Doucet, J.-P. *J. Chem. Res. (M)* **1980**, 1101–1129.
17. In a real molecule, these interatomic distances as well as those in Fig. 3 should be longer than the calculated values because the MM2 calculation underestimates the bending deformation of sp carbons. This trend is exemplified by the X-ray and MM2 structures of *ap*-**5b** and *ap*-**3** (Table 2).
18. Suzuki, A. *Pure Appl. Chem.* **1994**, *66*, 213–222.
19. Goldstein, A. E. *J. Am. Chem. Soc.* **1939**, *61*, 1600–1601.
20. Meyer, K. H. *Organic Syntheses*, Collective Volume I.; Gilman, H., Ed.; Wiley & Sons: New York; 1932, pp. 60–61.
21. Dickerman, S. C.; De Souza, D.; Wolf, P. *J. Org. Chem.* **1965**, *30*, 1981–1985.
22. Matsui, K.; Tobita, E.; Ando, M.; Kondo, K. *Chem. Lett.* **1981**, 1719–1720.
23. Gronowitz, S.; Hansen, G. *Ark. Kemi* **1967**, *27*, 145–151.
24. CHEM3D, Pro ver. 5.0; CambridgeSoft Corporation: Cambridge, MA, 1999.
25. Binsch, G. *Top. Stereochem.* **1968**, *3*, 97–192. Kleier, D.; Binsch, G. QCPE #165, Indiana University, Bloomington, IN, USA.